12th ICAS Congress
October 12-17,1980
München

Preprint of paper 13.2:

INFLUENCE OF JET LOCATION ON THE EFFICIENCY OF SPANWISE BLOWING *

by

W. STAUDACHER

MESSERSCHMITT-BÖLKOW-BLOHM GmbH
Unternehmensbereich Flugzeuge
Postfach 80 11 60
8000 München-Ottobrunn, West-Germany

ABSTRACT:

1. An experimental investigation was carried out to optimize the jet location for concentrated spanwise blowing over the wing upper surface. A systematic variation of 45 nozzle positions was performed, including jet locations in the body, over strakes, over the basic wing and over flaps and controls.

Optimum jet positions are determined in respect of improvements of

- performances
- stability
- control

2. An attempt was made to correlate the effects of spanwise blowing in lift- and drag development by an empirical approach based on POLHAMUS' Leading Edge Suction Analogy.

* this investigation was sponsored by the German Ministry of Defence (RüFo 4)

CONTENTS

1. SCOPE OF INVESTIGATION

This investigation is part of the coordinated efforts of a working group "Wings with Controlled Separation". The program was conducted by research institutes (DFVLR Göttingen and Braunschweig) and by industry (MBB, VFW) and was sponsored by the German Ministry of Defence. Part of the programme was performed in collaboration ONERA - MBB, see Ref. [2/5/8/9/10].

To create and manipulate this type of controlled separation, MBB took the experimental approach depicted in figure 1 (see also Ref. [2 to 13]), which is based on two different ways:

(1) Generation, control and stabilization of separated L.E. vortex systems via geometrical means, e.g. L.E. sweep, strakes, canards, fixes, trigger devices, section shape and L.E. flaps
⟶ planform and/or profile variations

(2) Make use of the technique of concentrated spanwise blowing, applicable on arbitrary wings, getting rid of the geometrical constraints in (1)
⟶ optimization of the nozzle position on the wing upper surface.

Both ways were investigated, since 1969 geometry based solutions were studied, since 1975 the effect on concentrated blowing was examined in the light of its applicability for controlled separation.

This paper deals mainly with the effectiveness of this latter technique in establishing this type of well organized separation and describes some results of the configurations investigated in respect of

- aerodynamic performances
- stability- and
- control-amplification

at low speed. It was decided from the beginning, that the investigation should be confined on low speed applications of spanwise blowing for the following reasons:

- spanwise blowing is a nonlinear technique regarding lift and drag development, tending to give the highest improvements at high angle of attack
- availability of excess thrust (≡ bleed air from the h.p. stage of the compressor) is restricted to the low speed regime, in addition the blowing intensity coefficient c_μ varies

$$c_\mu = \frac{\dot{m}\, v_{jet}}{\frac{\varrho}{2} V_\infty^2 \cdot S_{ref}} \succ \sim \frac{1}{M_\infty^2}$$

This is shown in more detail in Ref. [9].

2. MODELS AND APPARATUS

The model used is the MBB Low Speed Pilot Model being in service since 1970. Its geometry is shown in figure 2. The trapezoidal wing has an aspect ratio of AR = 3.2, the L.E. is swept back $\Lambda_{LE} = 32°$ and the planform is tapered $\lambda = 0.3$.

Basic section is NACA64A006 (root), varied over the span. The wing is cambered and twisted.
Additional modifications are

- Maneuver flap system
  - full span L. E. s l a t s ($c_f/c = 15\%$)
  - single slotted T. E. f l a p s with fowler extension ($c_f/c = 25\%$)
- Tip a i l e r o n s (1/3 of span)
- Detachable s t r a k e s (11% reference area), which can be replaced by c a n a r d s of same area.

The configuration incorporates an all moving horizontal tail for pitch and roll control and a conventional vertical tail with rudder.

The efficiency of the spanwise blowing technique was investigated in two test phases:

- In a first step blowing from the wing root was optimized. The nozzles were housed in the body side at five characteristic positions: 10% strake-wing root chord, 10/25/40% basic wing chord and one position over the T.E. flap (see fig. 2 bottom). Additionally nozzle sweep and nozzle height could be varied, combined blowing (synchronously operated strake and wing nozzles for the strake-wing e.g.) was tested also. Another variant was the blowing intensity c_μ, $0 \leq c_\mu \leq 0.4$. Results of this phase are reported in Ref. [6/7/9/10/13] and will not be treated in detail here.
- The remaining lack of systematic data for the effectivity of the spanwise blowing technique when using outboard nozzle positions, was eliminated in phase 2. A systematic variation of 41 outboard nozzle positions was conducted (figure 3):
  - 10/25/40/70% wing chord
  - 10/25/40/60/80% exposed span
  - 4 positions over the aileron
  - 17 positions in the strake region

  In both test phases basic and strake wing were examined, using the jet positions over the basic wing for the strake wing, too.

  The blowing system was always sting mounted (internal system in phase 1 and external system on only one half-wing in testphase 2) so, that mere aerodynamic interference effects were measured and jet reaction effects could not get on the internal 6-component strain gauge balance.

  Jet nozzles were of simple convergent type with 7.5 or 15mm ø, they were usually driven supercritically.

  The experimental data were derived from tests in the 3x3m low speed tunnel of DFVLR Göttingen.

3. EXPERIMENTAL RESULTS AND ANALYSIS *

We shall concentrate here on results found in the second test phase, all derived by blowing only on one wing half from outboard positions. This means, that all data are based on "asymmetric" conditions. It should be kept in mind that the here constant blowing coefficient $c_\mu = 0.1$ is refered to blown half wing area, being in contrast to the conventional notation. This inconsequence is tolerable as the statement for optimum jet location is not affected thereby.

3.1 Basic Aerodynamic Effects

Some principle effects of spanwise blowing are shown in figures 4 and 5, comparing the lift, - pitching moment - and drag development of the blown and unblown configuration.

Figure 4 shows the effect of spanwise variation of nozzle position (chordwise position 40% and nozzle sweep $\varphi_D = \Lambda_{LE}$ kept constant) for the basic wing without strake. Blowing efficiency is reduced for far outboard locations, giving less lift, less linearized pitching characteristics and a decrease in drag improvement at higher a.o.a.

The band-width of blowing efficiency for chordwise variation of the nozzle position on the basic wing is shown in figure 5 for the so far optimum spanwise position $\eta_{exp} = 0.1 = \text{const.}$ In addition the efficiency for blowing over the strake wing is given comparing optimum locations on the strake and on the basic wing.

Tendencies are the same for both wing types but demonstrating reduced efficiency of spanwise blowing for the strake wing with its "natural" tendency to develop stable separated L.E. vortex systems, thus shifting the "origin" of spanwise blowing to a higher level of nonlinearity at the expense of a lower gradient of efficiency (compare later to fig. 25 of § 4.1).

Figure 6 gives the effect of nozzle sweep for the a.o.a. regime investigated. Basic case for all locations was blowing parallel to the wing L.E. The insert chart demonstrates that maximum benefits are found for the most aft swept jet ($\Delta\varphi_D = 20°$ / $\varphi_{nozzle} = 52°$) for this specific location.

In figure 7 the lift/drag ratios at the first lift maximum (definition see insert chart of fig. 7) are shown to evaluate the improved performances due to this technique and its sensibility to variations of jet location in spanwise (top of fig. 7) and chordwise (bottom) directions.

Figure 8 compares the same criteria for comparable jet locations on strake and basic wing.
For the basic wing $\eta_{exp} = 0.1$ is used, for the strake wing the inner row (pos. 33/34/35/36/37, see fig. 3) is presented. Watch that the same criteria for $C_{L_{max}}$ is used for both wings but that these values are strongly different for strake ($C_{L_{max1}} = 1.2$, $\alpha_{max1} \approx 29°$) and basic wing ($C_{L_{max1}} \approx 0.8$, $\alpha_{max1} \approx 15°$) for non-blowing conditions.

---

* Part of the results have been reported in Ref. [13]

It is obvious that there is only about 2/3 of the absolute efficiency found on the strake wing relative to the basic wing expressed by $\Delta(L/D)_{c\mu}$, and that the strake wing is operating at more unfavourable conditions $(L/D)_{c\mu=0}$, but the relative efficiency, found by normalizing the (L/D)-ratios (fig. 8 bottom), is about the same for both wing types.

A summary of the basic beneficial effects of concentrated spanwise blowing is given in figure 9. Data for lift, drag and longitudinal stability were shown in figures 4 to 8, mentioned improvements for lateral/directional motion will be demonstrated later or have been reported in Ref. [2 to 13].

3.2 Optimum Nozzle Positions

For sake of completeness results of the optimization process for blowing from the wing root (testphase 1) are repeated in figure 10. Note that fig. 10 is presenting "true" data regarding now the maximum lift increment derived by symmetric blowing on the basic wing (at least twice the value as shown for comparison in fig. 6, insert chart, due to the changed convention for c_μ there). Optimum jet position was found for 40% root chord, a nozzle height of 1.5 ø and a blowing direction of 47° sweep back, that is $\Delta\varphi_D = 15°$ relative to the L.E.

The most insensitive parameter found was nozzle height, giving almost identical results when remaining between $1.0 \leq z_D/d \leq 2.5$. For that reason it was decided to keep the nozzle height constant at $z_D/d = 1.5$ for the second testphase, the data of which are presented in the following.

Results of the optimization process for outboard nozzle locations are given in the next two figures 11 and 12, now turning back again to asymmetric blowing with all the respective consequences in case of direct comparison of the two testphases.
Figure 11 is an equivalent to figure 10, using the same criteria $\Delta C_{L_{max}}$ due to blowing. The trace of the local optima (for constant chordwise cuts) is drawn in the wing plane (solid circles), demonstrating that the total optimum (big open circle) is found for blowing from the wing root, as already established in fig. 10.

Watch, that this is an as remarkable as non-typical result in the field of aerodynamics: The most simple system (in terms of weight, structure, mechanical supply, complexity etc.) is the aerodynamic most efficient one.

Local optimum nozzle positions for different criteria are depicted in figure 12. Most of the criteria used are representing high lift or high angle of attack cases as

- maximum induced lift increment $\Delta C_{L_{max}}$
- increase in lift/drag ratio at $C_{L_{max_1}} \cong \alpha_{max_1} = 15° \rightarrow \Delta(L/D)$
- lift increment at the same a.o.a. $\alpha_{max_1} \rightarrow \Delta C_{L_{max_1}}$

with one exception at low a.o.a.:

- optimum lift/drag-ratio $(L/D)_{opt}$

All optima are found to be localized between 10% and 40% chord. The spanwise gradients are found to be small for positions inboard 40% semispan (flat optimum) synchronously, so it can be stated that the best compromise is the place of wing-body intersection even for aerodynamic aspects alone.

Hence the formerly found optimum from the first test phase is reconfirmed (see fig. 10).

3.3 Center of Induced Lift

The spanwise position of the induced lift increment is found by division of the resulting rolling moment through the induced lift increment when applying spanwise blowing on one wing half only.

Figure 13 presents the induced rolling moment increments plotted against the respective lift increments for all nozzle positions investigated. The mean value (for $\alpha_{max_1} = 15°$) of all points is represented by the line through the origin, its gradient is the mean spanwise position $(\eta m)_{id}$ of the induced lift increment. This corresponds to a center of pressure at 47% exposed semispan. Additionally the check-probe standard error is marked as band width.

Figure 14 is the analogous picture for the strake wing, again giving the sample for α_{max} (but different incidence $\alpha_{max} = 27° > \alpha_{max_1} = 15°$) for blowing parallel to the basic wing L.E. The induced lift increment is now situated slightly more inboard ($\eta m_{exp} = 0.42$).

Figure 15 gives a visual aid in correlating the blowing locus (symbol +) with the respective center of induced lift (symbol •). Evidently there is a focusing near mid span independent of the spanwise nozzle position. Only extreme forward or rearward jet positions give a higher degree of departure to the rule tending to more outboard or inboard deviations, respectively.

3.4 Asymmetric Blowing and Roll Control

Spanwise concentrated blowing gives the possibility to improve the conventional roll control (aileron) twofold

- blowing over the aileron (or in its region) will improve the efficiency of this device at higher angles of attack, where its conventional characteristics will show the well known deficiencies ($\alpha > 15°$), when using positive (flap down) deflections,
- asymmetric blowing by itself will produce a non-linear increasing rolling moment due to the induced lift characteristics, controllable by nozzle sweep and/or blowing intensity c_μ.

As demonstrated in figure 16 it is more efficient to blow in front of the aileron than to blow over the knee of the (separated) plain flap, deflected 30° down.

Reorganizing the flow in the tip region of the wing gives additional profits relative to the pure restoring of the stalled aileron alone, now making use of the favourable forward induction of the aileron in unseparated flow. This positive interference aileron/spanwise blowing is analysed in figure 17, comparing the roll power of the aileron for the unblown case (curve ②), the effect of asymmetric blowing, aileron undeflected (curve ①) and the combined efficiency of blowing plus aileron deflection (curve ④). Curve ③ was derived by simply adding the values of curve ① and ②. Hence the difference between curves ④ and ③ is the favourable interference of concentrated blowing with the deflected aileron.

Generally spanwise blowing is less effective on the strake wing (see § 3.1 and fig. 5). This is manifested by figure 18 when compared with fig. 16, showing that for the strake wing the jet induced rolling moment increment $C_{l_{C_\mu}}$ is reduced. Neglecting the spike at $\alpha = 12°$ for blowing over the aileron knee, blowing parallel to the strake L.E. and blowing over the aileron give comparable results, in spite of the far inboard location of the jet (position ㉔), when blowing in the strake region. More details for that are presented in figure 19, demonstrating the effect of nozzle position on the induced rolling moment for cases blowing parallel to the strake L.E.

There is a definite trend of reduced efficiency for the b a c k w a r d- (outboard) orientated nozzle positions with a possible leveling for extreme a.o.a. (decay problem).

3.5 Summary and Conclusions

- Generally spanwise blowing is less efficient on wings, exhibiting a natural tendency to develop stable, separated L.E. vortex systems, as seen by the sample of the strake wing. Spanwise blowing is loosing its triggering (generating the separation) effect here and has to start from a higher level of nonlinearity, say vortex lift, then. Controlling and stabilizing an existing vortex system is more difficult and less effective, as there may be involved some perturbation effects for an existing condition of equilibrium in the flow.

  Nevertheless blowing on the strake wing with jet directions approximately equal to the L.E. sweep is attractive, as it offers system integrated effects of synergism (thrust and lift component of the jet). This is shown in detail in Ref. [9].

- Blowing from the wing root is the optimum compromise solution.

- Figure 20 is giving the optimum efficiencies of this blowing technique, dividing the maximum induced lift increment by the inducing blowing coefficient, which is a measure of superiority of the technique relative to a hovering jet ($\Delta C_L/c_\mu = 1$) for both wings in high lift configuration.

Effectivity of BLC techniques for two comparable contemporary fighters are drawn in. Efficiencies of both techniques are comparable but it should be kept in mind that BLC techniques tend to increase lift nearly independent of incidence, whilst spanwise blowing is basically increasing the lift at higher a.o.a. (and at the expense of higher incidences).

- There is a big amount of versatility offered by the technique of concentrated blowing to improve the maneuver capabilities directly and indirectly.
  Figure 21 is giving an overview of possible applications of the unique features of this simple technique.

4. EMPIRICAL CORRELATION

Trying to correlate the effects of spanwise blowing in an empirical way it was clear from the beginning, that the most simple and rapid approach should be based on POLHAMUS' Leading Edge Suction Analogy (Ref. [1]) when deriving the overall lift and drag coefficients for spanwise blowing.

There is a definite similarity in the resultant flow of wings exhibiting stable L.E. vortex systems due to their inherent, geometric characteristics (sweep, L.E. radius etc.) and the type of flow developed by concentrated blowing (especially from the wing root), replacing the lower geometrical sweep by a higher "effective" sweep due to jet entrainment effects. So POLHAMUS' analogy should hold for this case, too.

4.1 Extension of POLHAMUS L.E. Suction Analogy

POLHAMUS' basic reasoning when inventing the L.E. suction analogy, applicable to wings with L.E. separation of the afore mentioned type, may be summarized as follows (see figure 24)

- Modify the potential lift for higher angles of attack and for the condition of no flow around the (sharp) leading edge, introducing a KUTTA-condition on the L.E. → zero leading edge suction

  $\rightarrow C_{L_p} = K_p \sin\alpha \cos^2\alpha \quad (K_p = C_{L_\alpha})$

- The well organized vortex flow is inducing additional lift at the expense of lost L.E. suction. This exchange of for-

ces can be represented by a reorientation of this "lost" force called L.E. suction, turning it now perpendicular to the wing plane, giving a normal force increment and hence a lift increment → vortex lift

$$\rightarrow C_{L_V} = K_p\,(1 - K_p\,K_i)\,\frac{1}{\cos\Lambda_{LE}} \cdot \cos\alpha\,\sin^2\alpha \quad \left(K_i = \frac{\partial C_{D_L}}{\partial C_L{}^2}\right)$$

This vortex lift C_{L_V} was later extended by LAMAR to contributions of the side edge for tapered wings, and an "augmentation" part was introduced to count for the inducing effects of the developed vortex on surface behind. Note that pure means of potential theory are used contradictiously to represent separation effects.

To correlate the effects of spanwise blowing POLHAMUS' method has to be extended to count for the additionally found effects when applying concentrated blowing.

- "Quasi camber" effect at low a.o.a. in lift production → $\Delta C_{L_{c\mu}}$
- development of the jet induced, nonlinear vortex lift → $K_{v_{c\mu}}\cos\alpha\,\sin^2\alpha$

Analysing the experimental results found for the optimum jet locations on basic and strake wing, figures 22 and 23 were established, each representing the afore mentioned "quasi camber" effect $(\Delta C_{L_{c\mu}})_{\alpha=0}$ as a function of the applied blowing intensity c_μ; it was found that the effects of nozzle sweep, nozzle height and chordwise nozzle position are negligible when

- $0 \leq \Delta\varphi_D \leq 20$ nozzle sweep relative to L.E.
- $1.0 \leq \frac{z_D}{d} \leq 2.0$ nozzle height (ø above upper surface)
- $0.1 \leq \frac{x_D}{C_r} \leq 0.4$ nozzle chordwise position

Watch that there is a similar (but far less significant) trend found here with increasing c_μ as is well known from BLC techniques, when passing from boundary layer control to hyper-circulation, giving a rapid decrease in $\Delta C_L/\Delta c_\mu$.

This "quasi camber" term has to be corrected (see fig. 24) for higher a.o.a., so that

$$\Delta C_{L_{c\mu}} = \Delta(C_{L_{c\mu}})_{\alpha=0}\,(1 - K_k \cdot \alpha);\quad K_k \approx 2.0$$

as it was found easier to correct the "camber" term than the later developed vortex lift factor $K_{v_{c\mu}}$.

The factor K_k came out to be constant for all planforms investigated, it is sufficient to use $K_k = 2$.

The total jet/vortex induced effect is then represented by $\bar{K}_V = K_{v_{LE}} + K_{v_{SE}} + K_{v_{c\mu}}$ and is again found analysing the experimental data, shown in figure 25.

It is well understood that the basic wing without blowing does not exhibit a stable form of L.E. sparation (as anticipated when using

POLHAMUS' L.E. Analogy for this wing-type) but suffers (Λ_{LE} = 32°, ~ NACA64A006 section, AR = 3.2) from a long bubble type L.E. separation. Neglecting that and applying the original unextended method, giving $K_{v_{LE}} + K_{v_{SE}}$ for the basic wing, we find that a blowing intensity c_μ = 0.1 is necessary to generate this stable, organized type of L.E. separation as demonstrated in figure 25 by the constructing lines denoted "Basic wing".

Let now tend c_μ towards infiniteness. This would mean that the spanwise jet component will drive the tip vortices to infinite span, hence result in an infinite aspect ratio. Strictly applying the L.E. suction analogy this results in

$$K_{v_{c_\mu \to \infty}} = K_p \,(1 - K_p \cdot K_i)\, \frac{1}{\cos \Lambda_{LE}}$$

$$= 2\pi \,(1 - \cancel{2\pi \cdot 0})\, \frac{1}{\cos 32°} = \underline{7.40}$$

showing, that there is the same limit found when increasing the geometrical AR to infinite, say 2-dimensional conditions.

Figure 25 also can be used for wings, already exhibiting stable L.E. vortex systems as done here for a strake wing. Correcting $K_{v_{c_\mu}}$ for the "effected" area of the strake - as shown in fig. 24, bottom - the same formula may be applied, when one takes into account, that the "natural" vorticity effect has to be subtracted ($K_{v_{LE_{Str.}}}$) in fig. 25 from the total $\bar{K}_v$. This means that one only has to shift the origin to the (calculated or measured) value of $K_{v_{LE_{Strake}}}$, and counting c_μ from there, as denoted in fig. 25. Note that the blowing efficiency (in terms of $K_{v_{c_\mu}}$) is ~ 3.3 for the basic wing and 2.2 for the strake wing, for a constant c_μ = 0.1, but that the total vortex lift (in terms of $\bar{K}_v$) is 3.9 : 3.3 in favour of the strake wing. Figure 25 is of course applicable for a delta wing, too, one only has to apply the strake wing procedure, setting F_{Strake}/F_{eff} = 1. $K_{v_{LE}}$ can be calculated easily or taken from experimental results.

4.2 Examples

Figure 26 gives direct comparisons experiment/calculation after the extended L.E. Suction Analogy, including the unblown case c_μ = 0, for lift and drag characteristics. Induced drag is easily determined when the lift characteristics are established:

$$C_{D_L} = C_L \tan\alpha \quad \text{(zero L.E. suction)}$$

$$\succ (\Delta C_{D_L})_{c_\mu} = \bar{K}_{v_{c_\mu}} \sin^2\alpha \cos\alpha + \left[(\Delta C_{A_{c_\mu}})_{\alpha=0} \,(1 - K_k \alpha) \right] \tan\alpha$$

As expected, agreement theory/experiment is excellent, as the correlation is based on the experimental results of this wing and so far not giving any proof for the general validity of the method.

Figure 27 demonstrates that the extended method will provide similar good agreement for the strake wing, when using the before mentioned

modified approach. The lift increments due to blowing for zero incidence $(\Delta C_{L_{C\mu}})_{\alpha=0}$ were taken from figure 23.

As a last example figure 28 presents experimental data from Ref. [3] for a delta wing configuration, when blowing from the optimum position of the nozzle found for this wing. The planform (Λ_{LE} = 50.5° / AR = 3.15 / λ = 0.026) nearly does not develop a L.E. vortex system, as can be seen by the small amount of nonlinear lift production ($K_{v_{LE}}$ = 0.37). Using this value as starting position $K_{v_{C\mu=0.1}}$ = 2.9 was derived from fig. 25, $(\Delta C_{L_{C\mu}})_{\alpha=0}$ was taken from fig. 23. Again the agreement is good, demonstrating the general applicability of the established method and the high degree of efficiency of POLHAMUS L.E. suction analogy.

5. REFERENCES (direct)

[1] POLHAMUS E.C.
A concept of the Vortex Lift of Sharp-Edge Delta Wings Based on a Leading-Edge-Suction Analogy
NASA TN D-3767 1966

[2] STAUDACHER W. / HONECKE K.
Flügel mit und ohne Strakes im Post-Stall-Bereich
Gemeinschaftsarbeit MBB-UFE 1300 / VF Ef-652 ZTL 1967

[3] HONECKE K. / KRAHL H.
Grundsatzuntersuchungen über spannweitiges Ausblasen
VFW-F KB Ef-626/782 1976/78

[4] STAUDACHER W.
The Effects of Jets, Wakes and Vortices on Lifting Surfaces
AGARD FDP RTD / MBB-UFE122-AERO-MT-263 1976

[5] LEDY J.P. / TURBIL R.
Essai d'une maquette complète d'un avion de combat MBB, a l'échelle 1/5.5, avec jets transversaux, dans la veine d'expérience no 1 de la soufflerie S1MA
Procès-verbal no 2/3302 SNG 1977

[6] STAUDACHER W./BÖDDENER W./WULF R.
Grundsätzliche Untersuchungen über spannweitiges Ausblasen und stabilisierten Widerstand
Gemeinschaftsarbeit MBB-UFE 1320 / DFVLR IB 157-77A25 RüFo 1977

[7] STAUDACHER W.
Flügel mit kontrollierter Ablösung
MBB-UFE1343(Ö) / DGLR Nr. 77-028 1977

[8] STAUDACHER W./LASCHKA B./SCHULZE B./POISSON-QUINTON Ph./CANU M.
Some Factors Affecting the Dynamic Stability Derivatives of a Fighter-Type Model
AGARD FDP Athens, May 1978, Paper 11 1978

[9] STAUDACHER W./LASCHKA B./POISSON-QUINTON Ph./LEDY J.P.
Effect of Spanwise Blowing in the Angle-of-Attack Regime $\alpha = 0 \div 90°$
ICAS A1-02, Lisboa 1978

[10] STAUDACHER W./LASCHKA B./POISSON-QUINTON Ph./LEDY J.P.
Aerodynamic Characteristics of a Fighter-Type Configuration During and Beyond Stall
AGARD CP 247, Paper 8 1978

[11] STAUDACHER
Kontrollierte Ablösung durch Spannweitiges Ausblasen
DGLR Symp. "Strömungen mit Ablösungen" 1979

[12] STAUDACHER W./STIEB R./BÖDDENER W.
Verbesserung der aerodynamischen Leistungen durch konzentriertes Ausblasen
MBB/S/R/1499 RüFo 1980

[13] STAUDACHER W.
Interference Effects of Concentrated Blowing and Vortices on a Typical Fighter Configuration
AGARD Paper 19-1, München 5-7 May 1980

REFERENCES (related)

[14] DIXON C.J.
Lift Augmentation by Lateral Blowing over a Lifting Surface
AIAA No. 69-193 1969

[15] CORNISH J.J. III
High Lift Application of Spanwise Blowing
ICAS Paper No. 70-09 1970

[16] DIXON C.J.
Lift and Control Augmentation by Spanwise Blowing over Trailing Edge Flaps and Control Surfaces
AIAA Paper No. 72-781 1972

[17] BRADLEY R.G./SMITH C.W./BHATELEY I.C.
Vortex-Lift Prediction for Complex Wing Planforms
J. Aircraft Vol.10 No.6 1973

[18] BRADELEY R.G./WRAY W.O.
A Conceptional Study of Leading-Edge Vortex Enhancement by Blowing
AIAA Paper No. 73-656 1973

[19] BRADLEY R.G./SMITH C.W./WRAY W.O.
An Experimental Investigation of Leading-Edge Vortex Augmentation by Blowing
NASA CR-132515 1974

[20] CAMPBELL J.F.
Effects of Spanwise Blowing on the Pressure Field and Vortex-Lift Characteristics of a 44° Swept Trapezoidal Wing
NASA TN-D 7907

[21] BRADLEY R.G./WHITTEN P.D./WRAY W.O.
Leading-Edge Vortex Augmentation in Compressible Flow
AIAA Paper No. 75-124 1975

[22] KNORR G.
Experimenteller Vergleich zweier Ausblaskonzepte am Modell eines leichten STOL-Flugzeuges
TU Braunschweig, Studienarbeit 1975

[23] JENKINS M.W.M. / MEY R.T.
A Large-Scale Low-Speed Tunnel Test of a Canard Configuration with Spanwise Blowing
AIAA Paper No. 75-994 1975

[24] CAMPBELL J.R.
Augmentation of Vortex Lift by Spanwise Blowing
AIAA Paper No. 75-993 1975

[25] NUGMANOV H.Kh.
Experimental Study of Spanwise Airjet Influence on Wing Aerodynamic Characteristics
Izvestiya VUZ. Aviatsionnaya Tekhnika 1976

[26] KRUPPA E.W.
A Wind Tunnel Investigation of the KASPER Vortex Concept
AIAA Paper No. 77-310 1977

[27] DIXON C.J./DANSBY T./POISSON-QUINTON Ph.
Benefits of Spanwise Blowing at Transonic Speeds
ICAS Paper No. A1-01, Lisboa 1978

[28] CORNISH J.J. / JENKINS M.W.M.
The Application of Spanwise Blowing for High Angle of Attack Spin Recovery
AGARD CP 247, Paper 9 1978

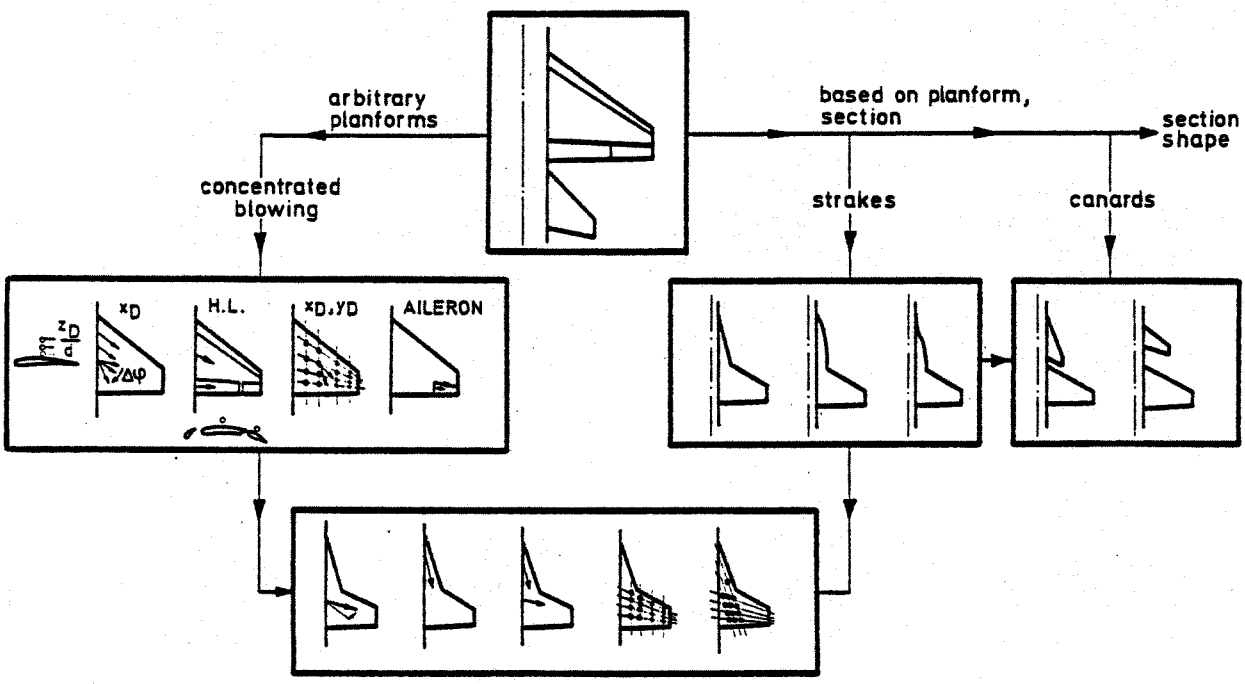

FIG. 1 EXPERIMENTAL APPROACH
FOR WINGS WITH CONTROLLED SEPARATION

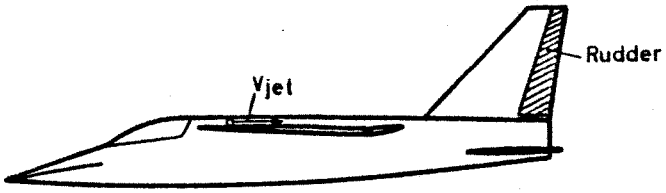

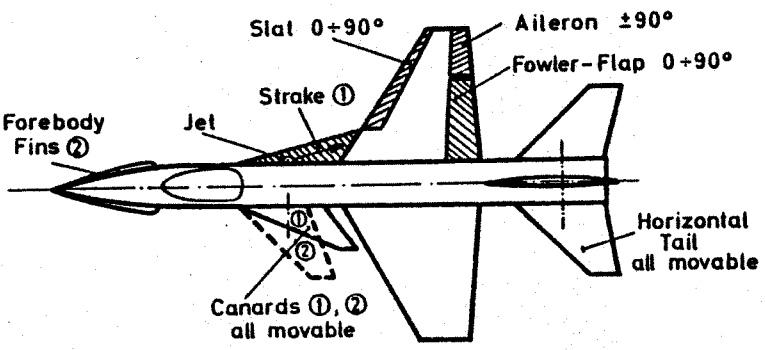

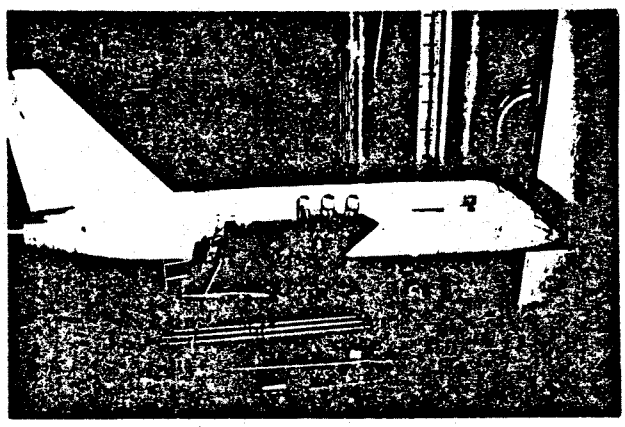

3x3 m L.S. Tunnel, DFVLR Göttingen

FIG. 2 PILOT MODEL

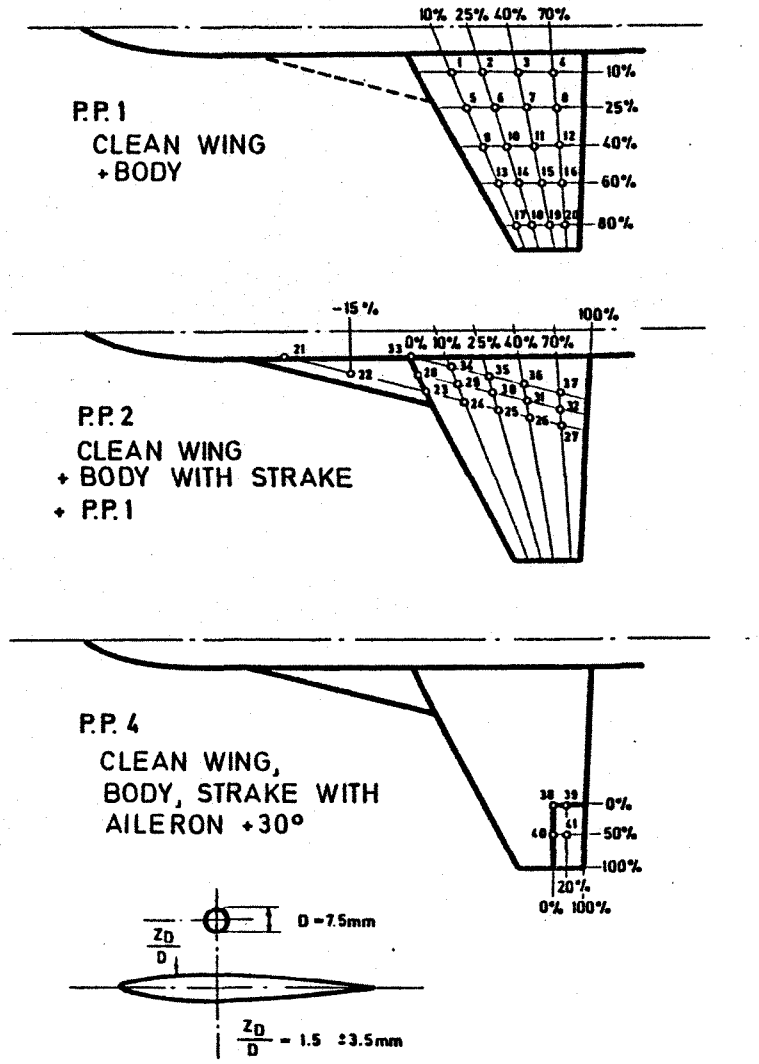

FIG. 3 TESTED NOZZLE POSITIONS

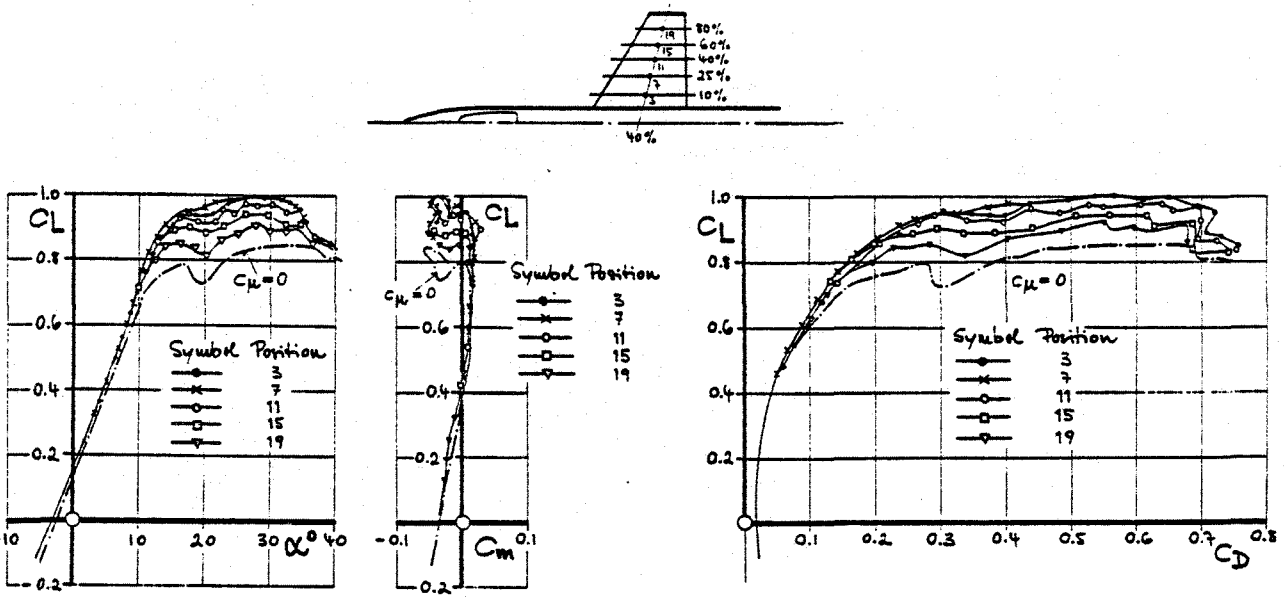

FIG. 4 EFFECT OF SPANWISE NOZZLE LOCATION ON LIFT, PITCHING MOMENT AND DRAG

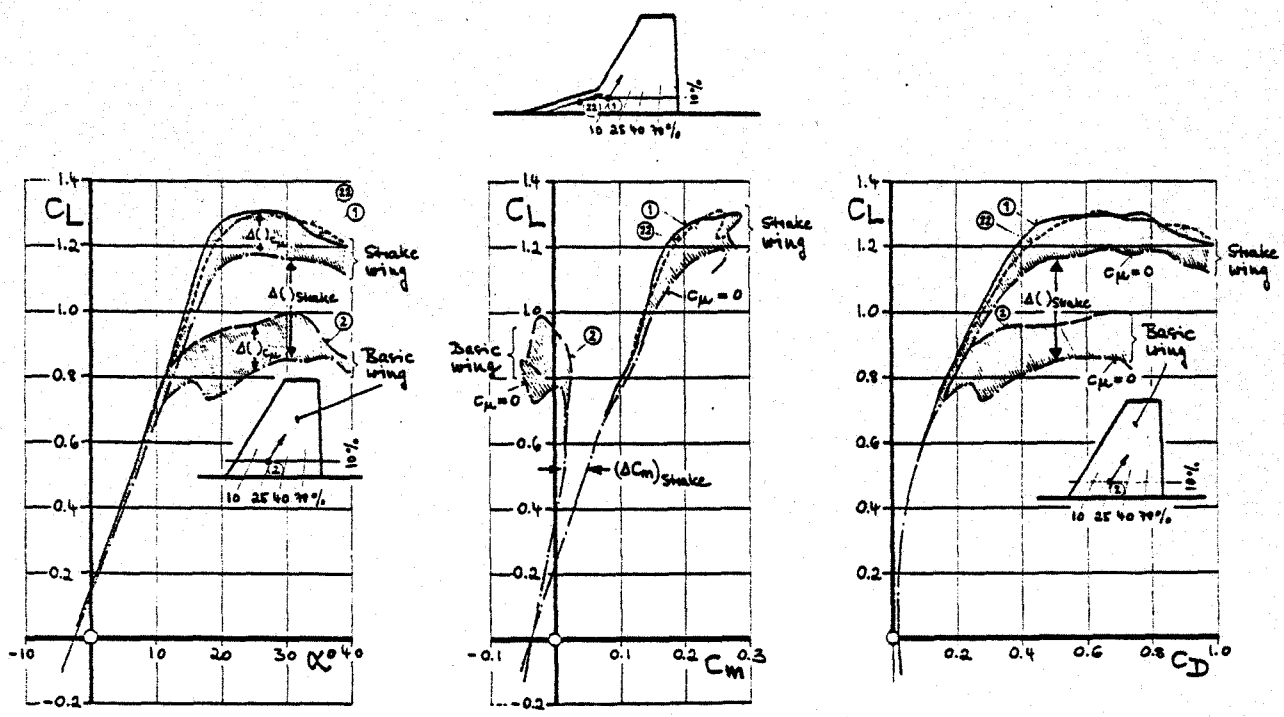

FIG. 5 OPTIMUM NOZZLE LOCATIONS: COMPARISON OF WING-PLANFORMS

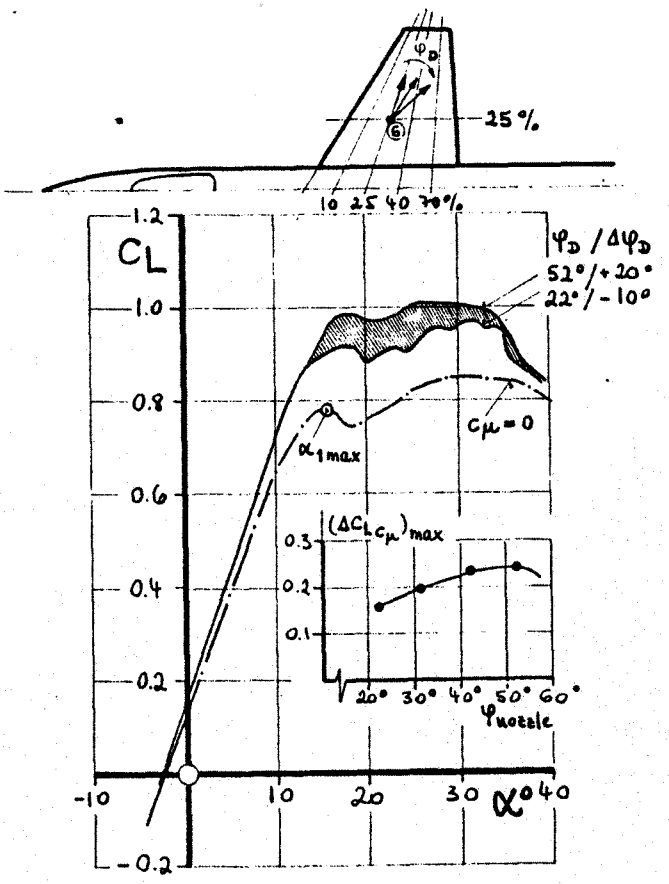

FIG. 6 EFFECT OF NOZZLE-SWEEP

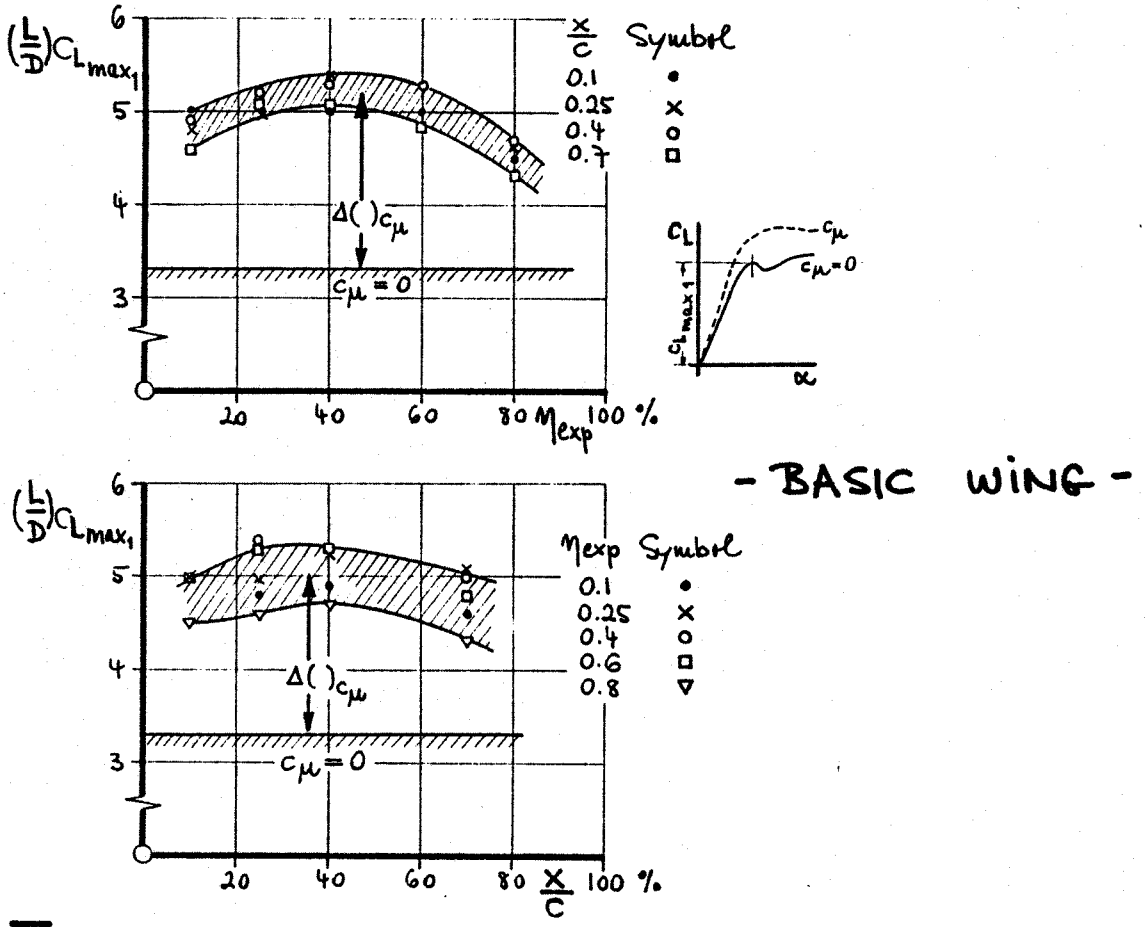

FIG. 7 EFFECT OF NOZZLE - -LOCATION ON L/D-RATIOS AT FIRST LIFT-MAXIMUM

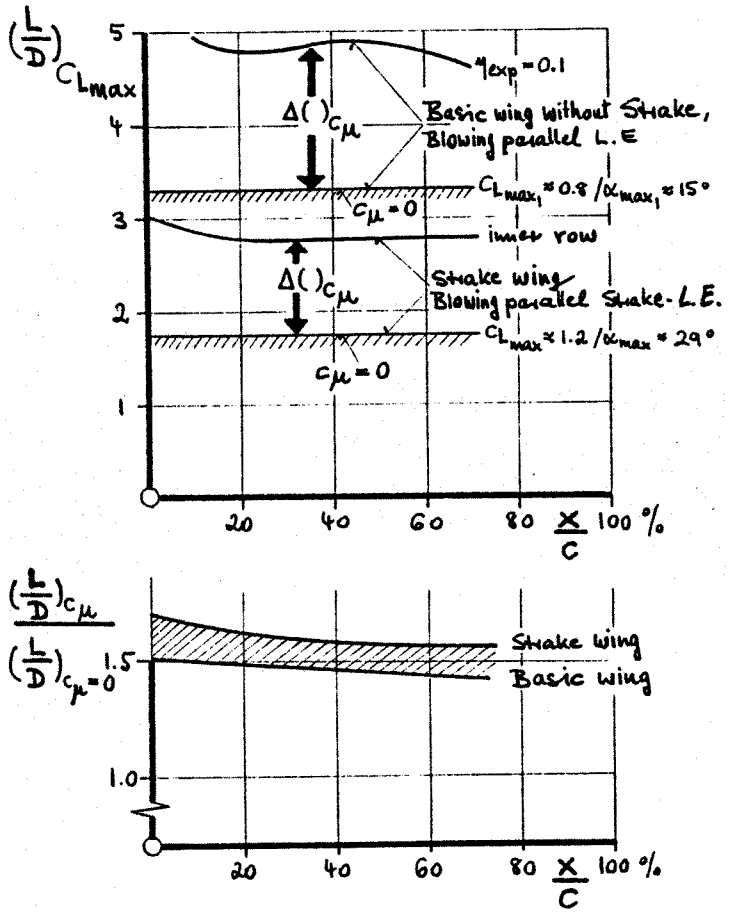

FIG. 8 COMPARISON OF L/D-RATIOS ON BASIC- AND STRAKE WING FOR MAXIMUM LIFT

- Lift Production:
  - quasi camber effect at low α
  - nonlinear increase of jet/vortex-induced lift with increasing a.o.a. and blowing intensity
  - increased $C_{L_{max}}$ and α_{max}

- Drag Development:
  - reduced lift dependent drag at higher incidences due to reduced a.o.a. for constant C_L: $\Delta C_D = -C_L(\tan \alpha_{C_\mu=0} - \tan \alpha_{C_\mu})$
  - less trim drag

- Longitudinal Stability:
  - linearized pitching characteristics at high a.o.a. (reduced pitch-up or-down characteristics)
  - basic stability (neutral point) and zero-pitching moment (center of pressure) unchanged

- Lateral / Directionals:
  - increase of effective dihedral and directional stability and controllability at high a.o.a. by either direct effects (improved flow on the wing) or indirect effects (improved conditions in the wing wake = reduced side wash and increased dynamic pressure)

FIG. 9 BASIC BENEFICIAL EFFECTS OF CONCENTRATED SPANWISE BLOWING

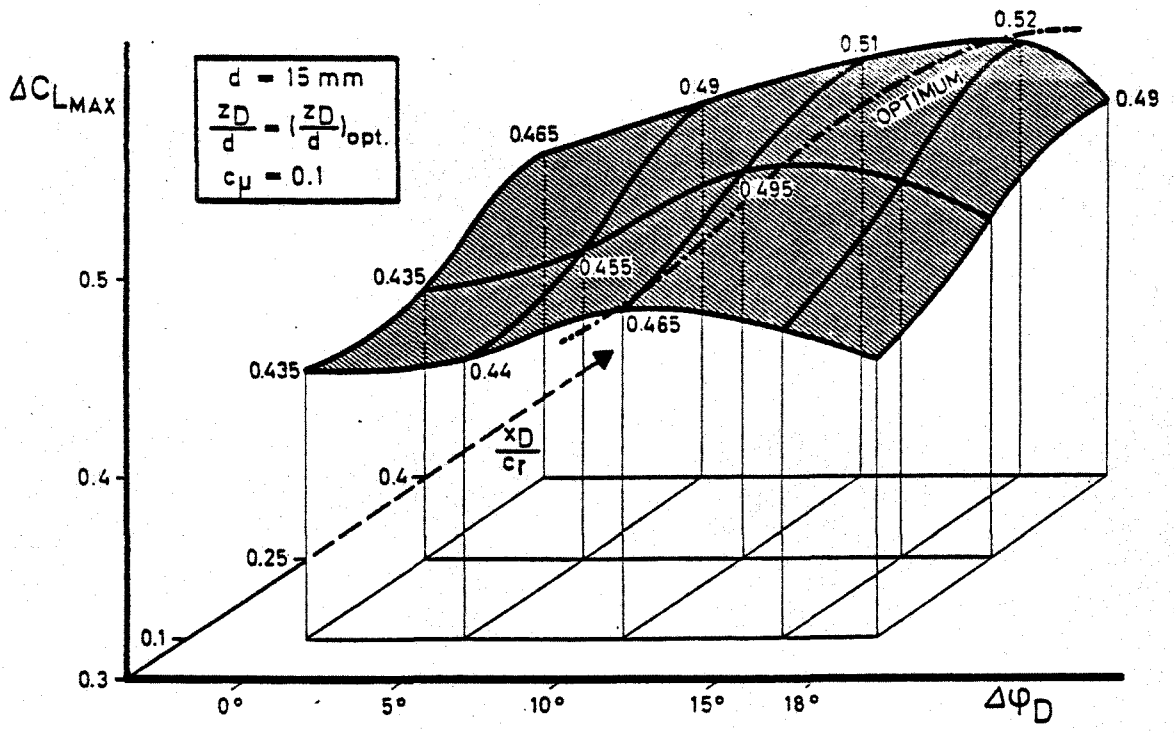

FIG. 10 OPTIMIZATION OF JET POSITION AND DIRECTION (blowing from the wing root)

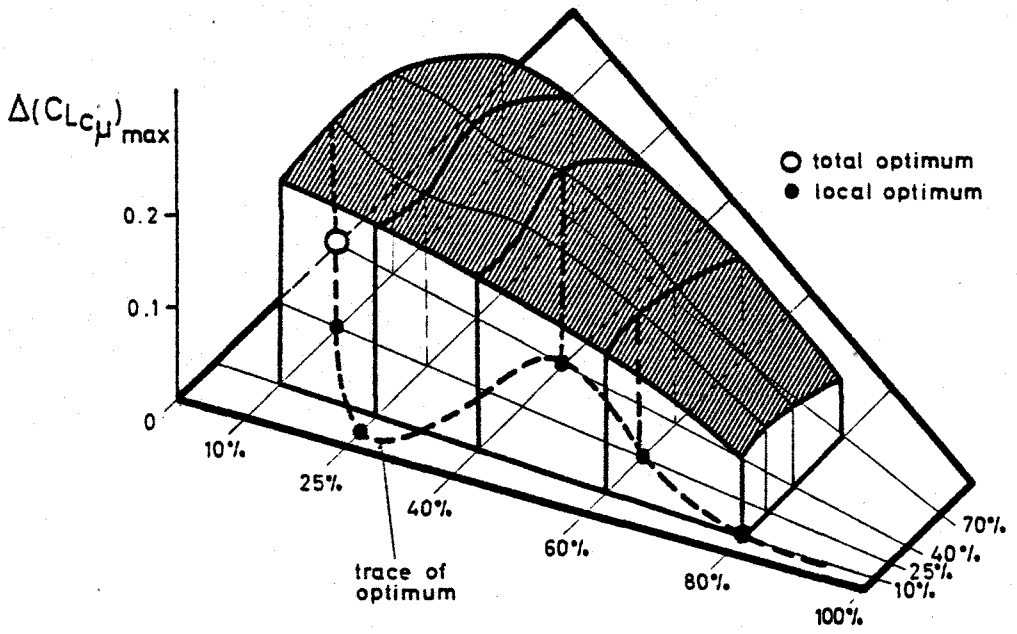

FIG. 11 EFFECT OF NOZZLE POSITION ON OUTBOARD WING

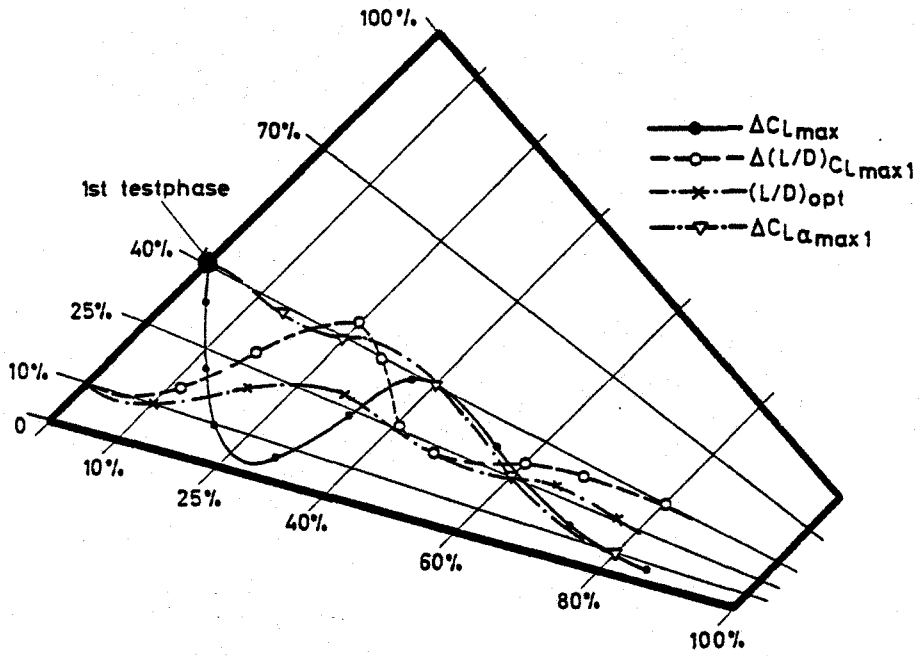

FIG. 12 LOCAL OPTIMUM POSITIONS FOR DIFFERENT CRITERIA

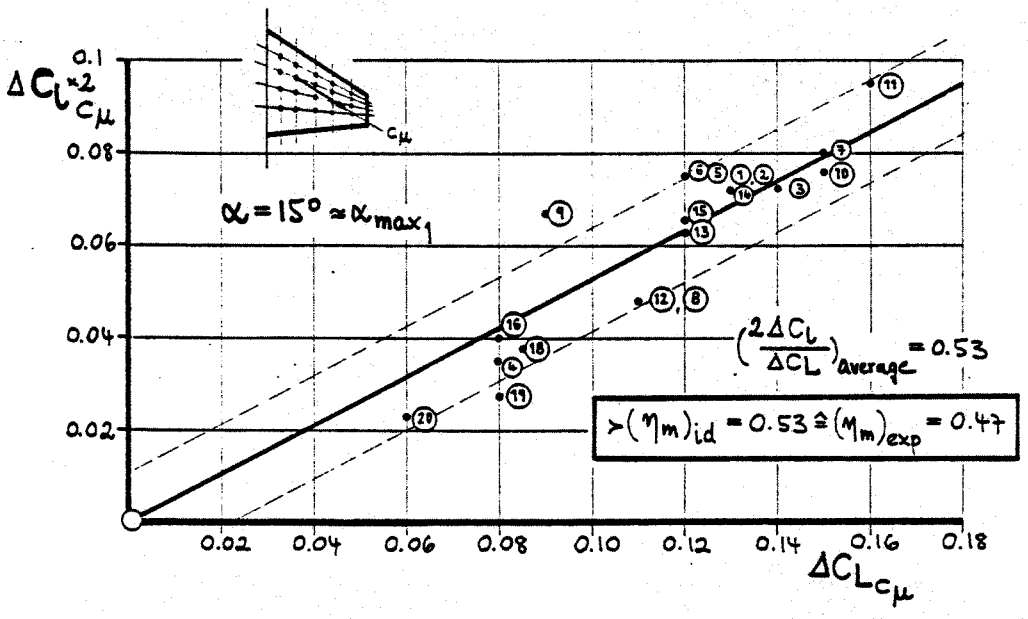

FIG. 13 INDUCED ROLLING MOMENT AND LIFT INCREMENT DUE TO ASYMMETRIC SPANWISE BLOWING ON BASIC WING

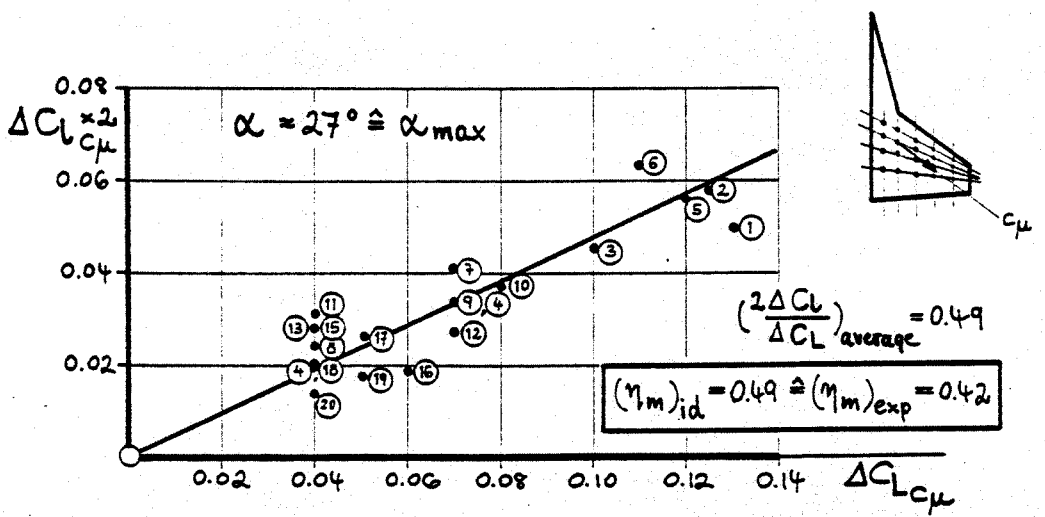

FIG. 14 INDUCED ROLLING MOMENT AND LIFT INCREMENT DUE TO ASYMMETRIC SPANWISE BLOWING ON STRAKE WING

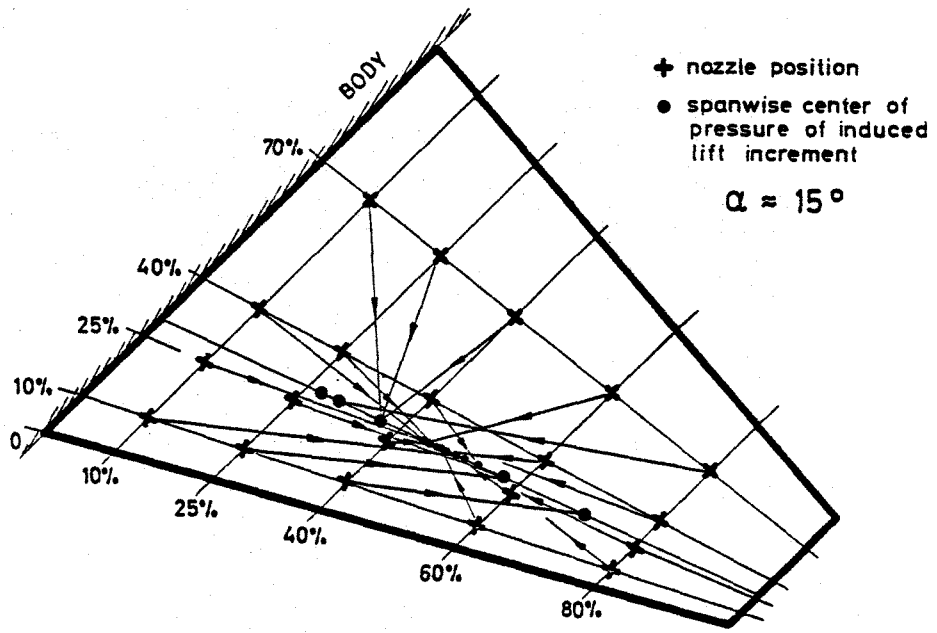

FIG. 15 NOZZLE POSITION AND CENTER OF INDUCED LIFT INCREMENT AS DERIVED BY ASYMMETRIC BLOWING

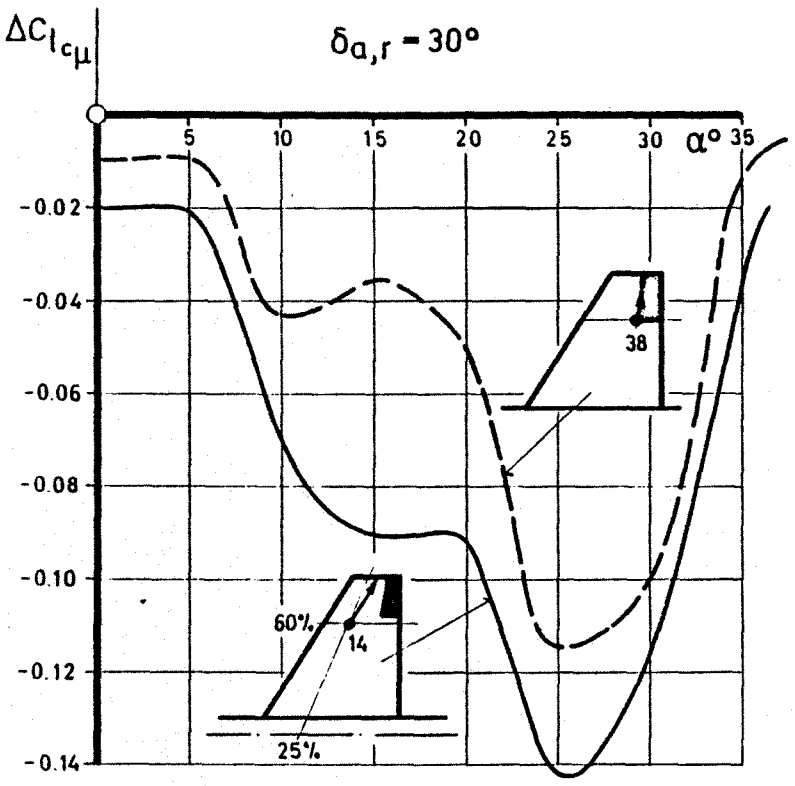

FIG. 16 EFFECT OF JET POSITION ON AILERON POWER

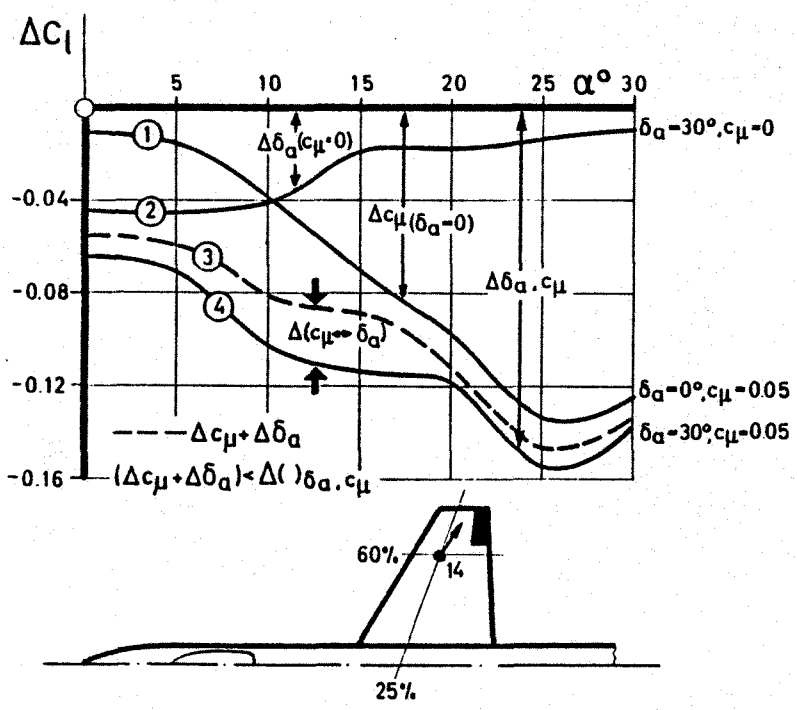

FIG. 17 ROLL POWER DUE TO AILERON AND/OR SPANWISE BLOWING

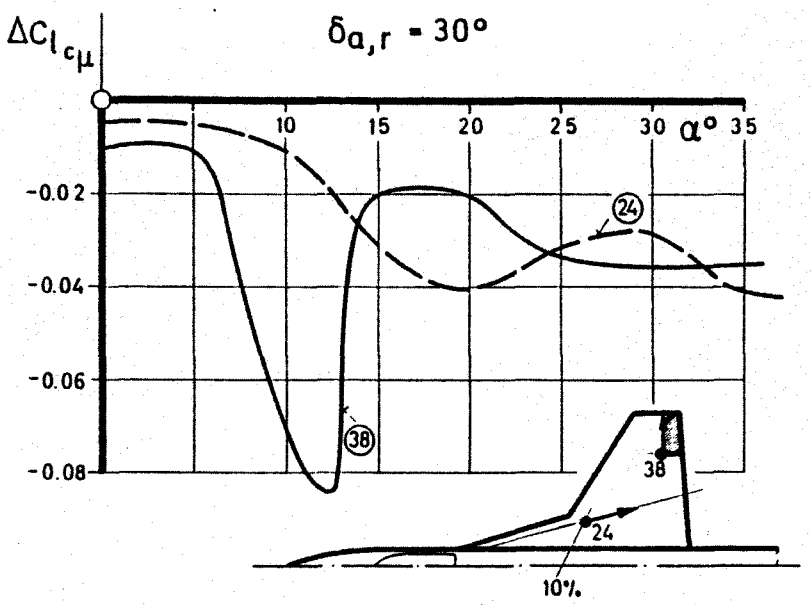

FIG. 18 EFFECT OF CONCENTRATED BLOWING ON AILERON POWER (STRAKE WING)

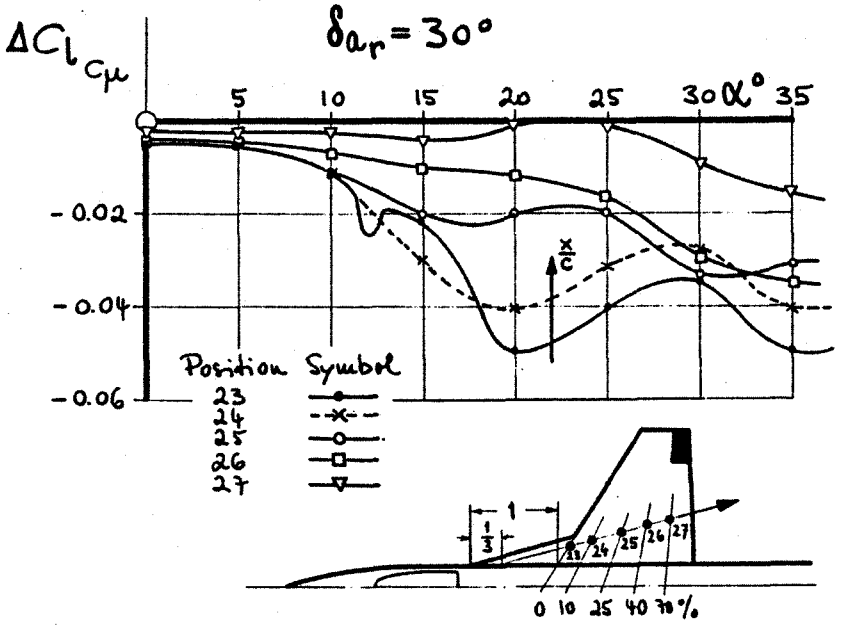

FIG. 19 EFFECT OF AILERON-ROLL-POWER (NOZZLE DIRECTION: PARALLEL STRAKE L.E.)

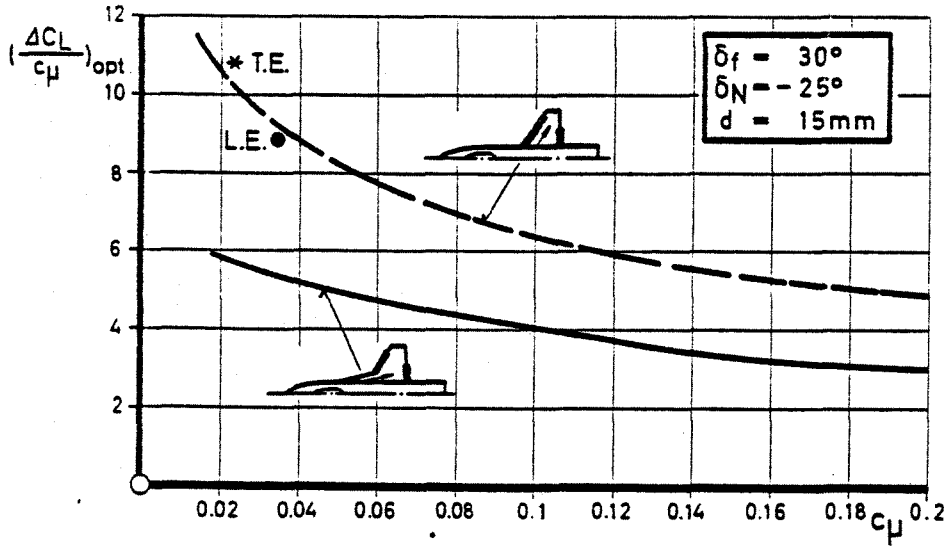

FIG. 20 BLOWING EFFICIENCY ON HIGH LIFT CONFIGURATION (*, ● BLC ON CONTEMPORARY FIGHTERS)

BLOWING OVER LIFTING SURFACES

- increased maximum lift
- reduced drag level at high angle of attack
- improved roll control
  - aileron efficiency
  - asymmetric blowing
- higher maneuver limits
  - buffet
  - stability (reduction of a.c.-shift)
  - reduction of spin susceptibility (C_{l_β} improved)

BLOWING OVER CONTROLS

- increased efficiency
- spin prevention or recovery (aileron, rudder, vertical tail)

BLOWING OVER THE FOREBODY

- control of vortex shedding
- departure prevention

FIG. 21 EFFECTS OF SPANWISE BLOWING IN THE SUBSONIC (TRANSONIC) FLIGHT REGIME

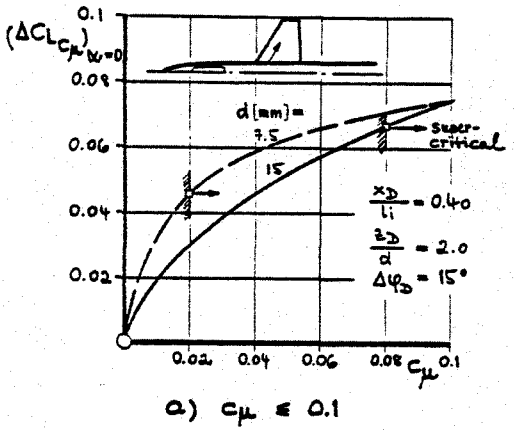

a) $C_\mu \leq 0.1$

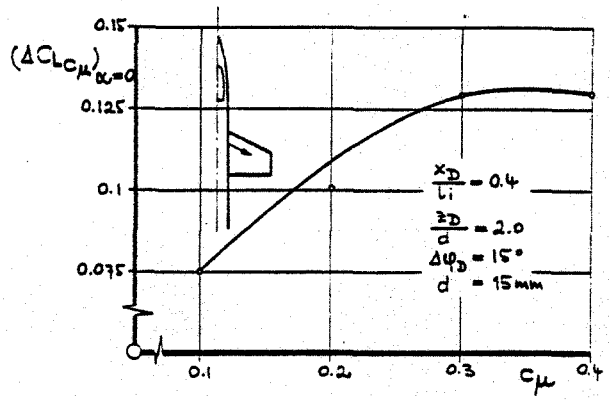

b) $C_\mu \geq 0.1$

FIG. 22 QUASI-CAMBER-EFFECT OF CONCENTRATED BLOWING ON TRAPEZOIDAL WING

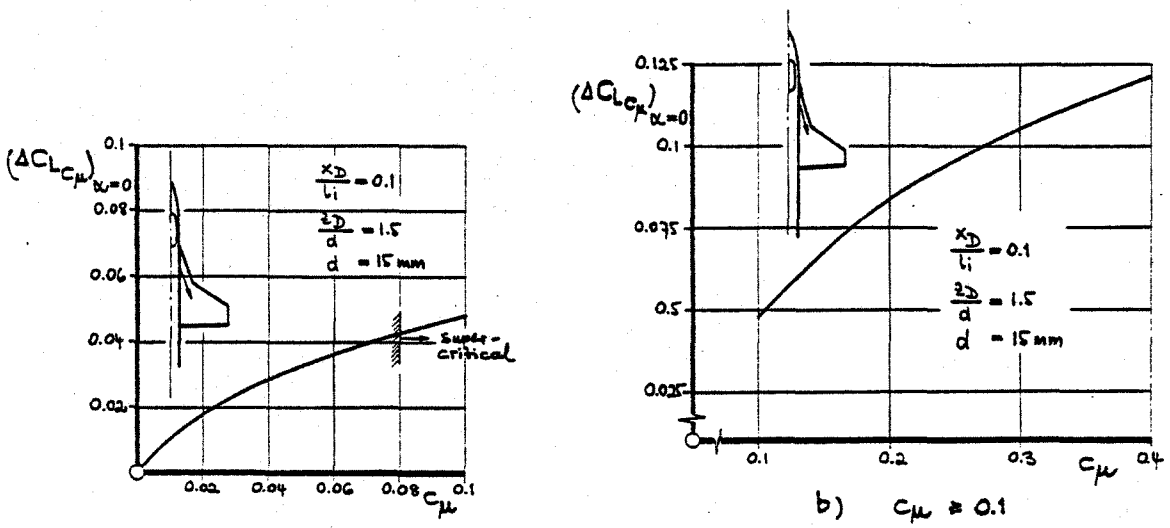

FIG. 23 QUASI-CAMBER-EFFECT OF CONCENTRATED BLOWING ON STRAKE WING

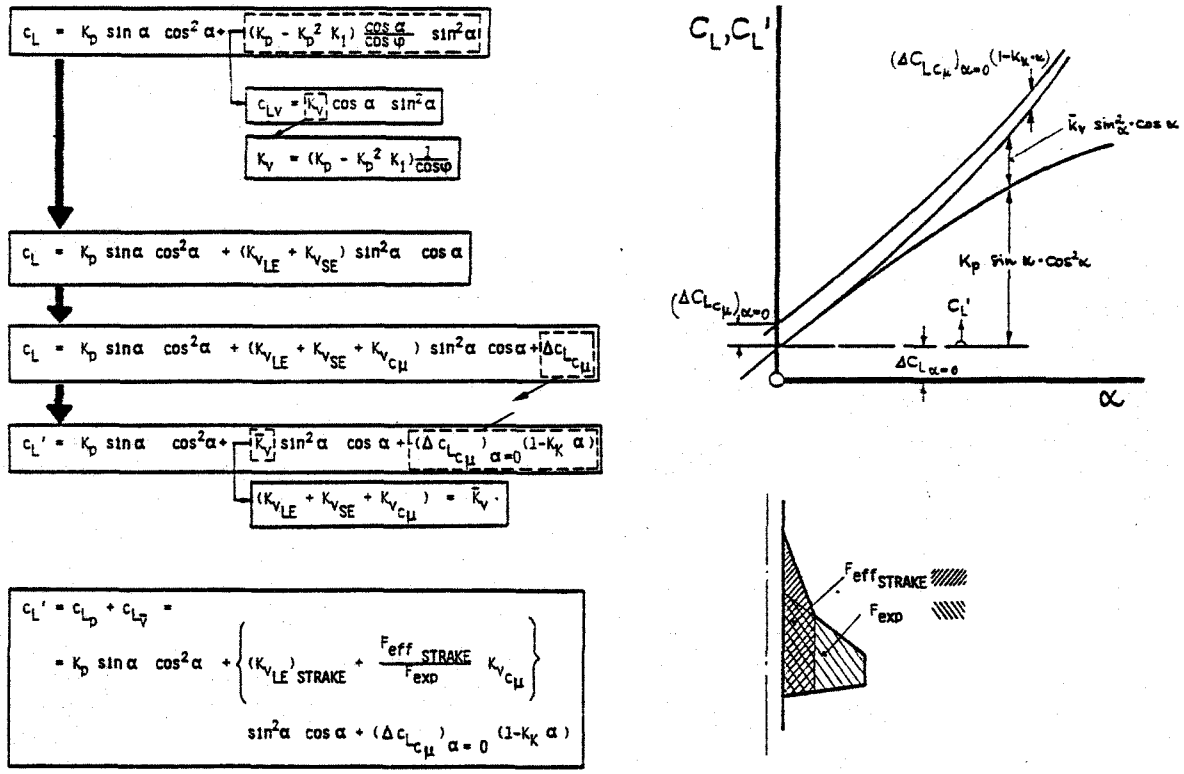

FIG. 24 EXTENSION OF L.E. SUCTION ANALOGY FOR SPANWISE CONCENTRATED BLOWING

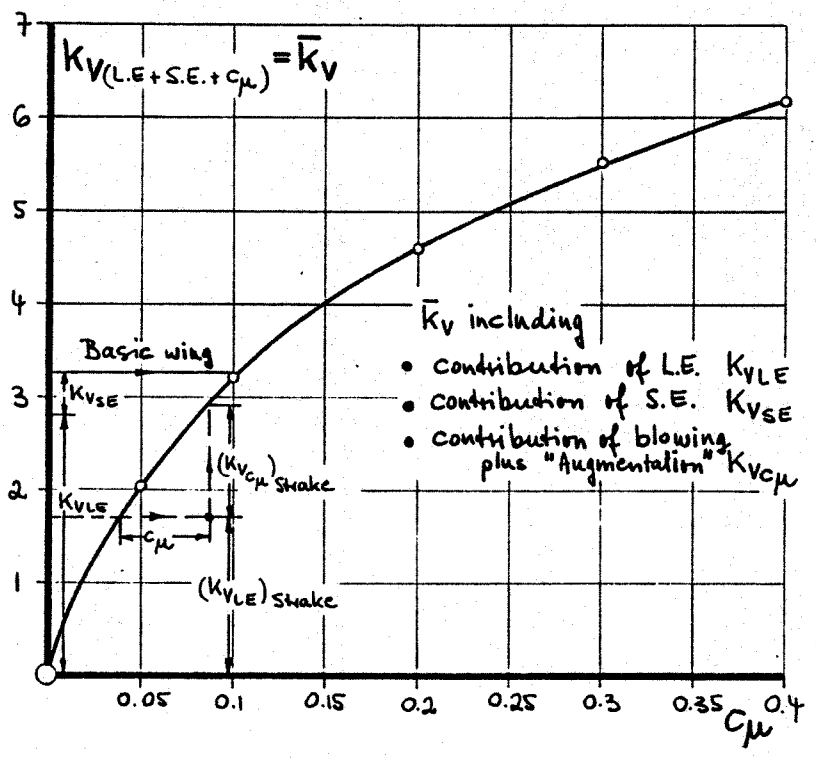

FIG. 25 FACTOR OF TOTAL VORTEX-INDUCED LIFT INCLUDING SPANWISE BLOWING EFFECTS

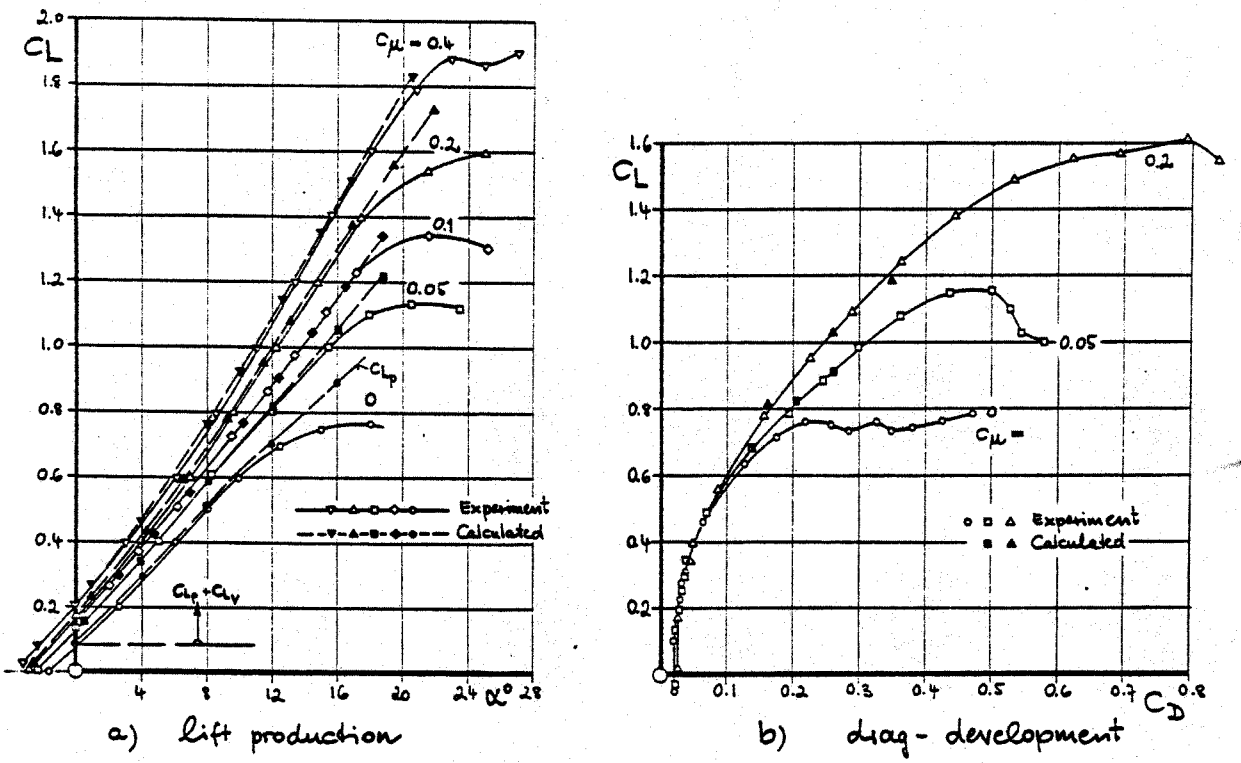

FIG. 26 COMPARISON EXPERIMENT / CALCULATION FOR BASIC TRAPEZOIDAL WING

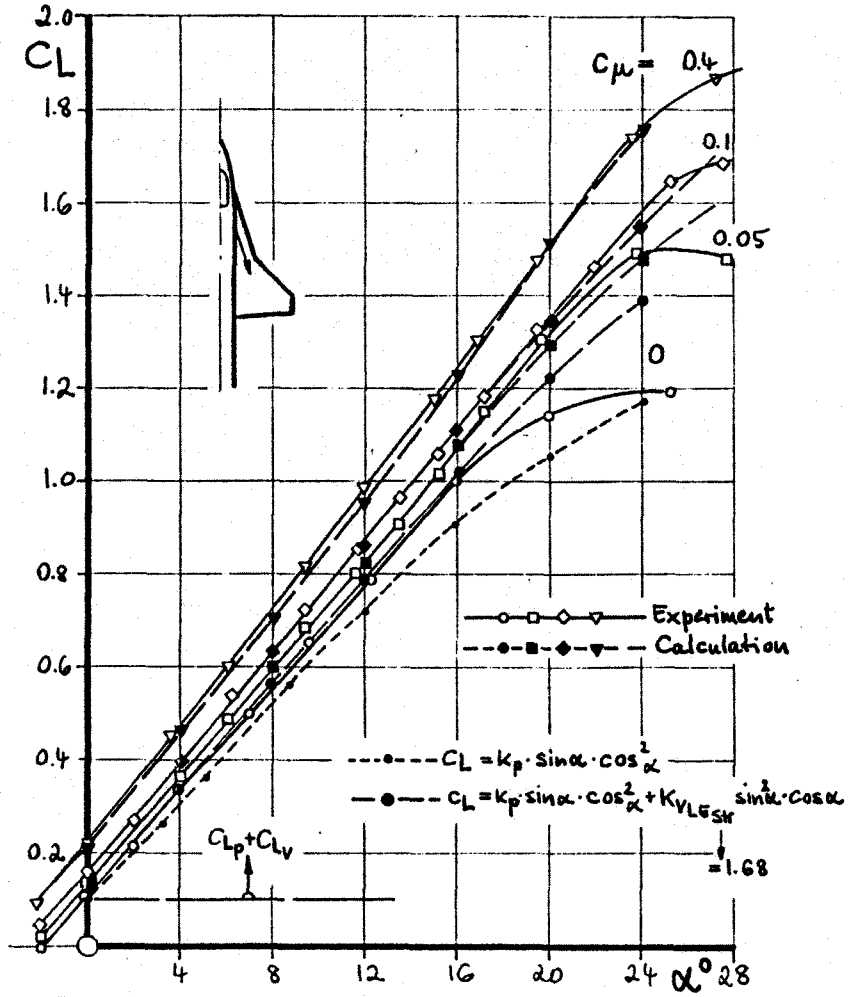

FIG. 27 COMPARISON EXPERIMENT/CALCULATION FOR STRAKE WING

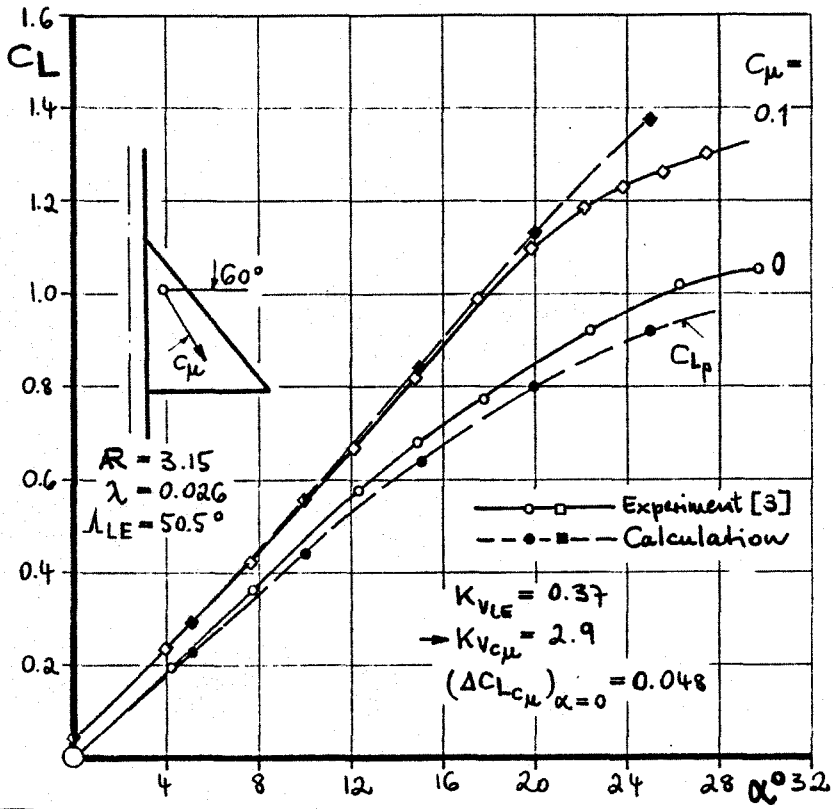

FIG. 28 COMPARISON EXPERIMENT / CALCULATION FOR A DELTA WING CONFIGURATION